### The Emission Coefficient

In the following discussions of beams and light rays, the primary consideration is the net flow of energy in a given direction, not the specific path taken by individual photons. First, we will examine the emission process that increases the intensity of a ray of wavelength $\lambda$ as it travels through a gas. The increase in intensity $dI_\lambda$ is proportional to both $ds$, the distance traveled in the direction of the ray, and $\rho$, the density of the gas. For pure emission (no absorption of the radiation),

$$dI_\lambda = j_\lambda \rho \, ds, \tag{9.32}$$

where $j_\lambda$ is the **emission coefficient** of the gas. The emission coefficient, which has units of m $s^{-3}$ $sr^{-1}$, varies with the wavelength of the light.

As a beam of light moves through the gas in a star, its specific intensity, $I_\lambda$, changes as photons traveling with the beam are removed by absorption or scattering out of the beam, and are replaced by photons emitted from the surrounding stellar material, or scattered into the beam. Combining Eq. (9.13) for the decrease in intensity due to the absorption of radiation with Eq. (9.32) for the increase produced by emission gives the general result

$$dI_\lambda = -\kappa_\lambda \rho I_\lambda \, ds + j_\lambda \rho \, ds. \tag{9.33}$$

The ratio of the rates at which the competing processes of emission and absorption occur determines how rapidly the intensity of the beam changes. This is similar to describing the flow of traffic on an interstate highway. Imagine following a group of cars as they leave Los Angeles, traveling north on I-15. Initially, nearly all of the cars on the road have California license plates. Driving north, the number of cars on the road declines as more individuals exit than enter the highway. Eventually approaching Las Vegas, the number of cars on the road increases again, but now the surrounding cars bear Nevada license plates. Continuing onward, the traffic fluctuates as the license plates eventually change to those of Utah, Idaho, and Montana. Most of the cars have the plates of the state they are in, with a few cars from neighboring states and even fewer from more distant locales. At any point along the way, the number of cars on the road reflects the local population density. Of course, this is to be expected; the surrounding area is the source of the traffic entering the highway, and the rate at which the traffic changes is determined by the ratio of the number of entering to exiting automobiles. This ratio determines how rapidly the cars on the road from elsewhere are replaced by the cars belonging to the local population. Thus the traffic constantly changes, always tending to resemble the number and types of automobiles driven by the people living nearby.

### The Source Function and the Transfer Equation

In a stellar atmosphere or interior, the same considerations describe the competition between the rates at which photons are plucked out of a beam of light by absorption, and introduced into the beam by emission processes. The ratio of the rates of emission and absorption determines how rapidly the intensity of the beam of light changes and describes the tendency of the population of photons in the beam to resemble the local source of photons in the surrounding stellar material. To introduce the ratio of emission to absorption, we divide

Eq. (9.33) by $-\kappa_\lambda \rho\, ds$:

$$-\frac{1}{\kappa_\lambda \rho}\frac{dI_\lambda}{ds} = I_\lambda - \frac{j_\lambda}{\kappa_\lambda}.$$

The ratio of the emission coefficient to the absorption coefficient is called the **source function**, $S_\lambda \equiv j_\lambda/\kappa_\lambda$. It describes how photons originally traveling with the beam are removed and replaced by photons from the surrounding gas.[23] The source function, $S_\lambda$, has the same units as the intensity, W m$^{-3}$ sr$^{-1}$. Therefore, in terms of the source function,

$$\boxed{-\frac{1}{\kappa_\lambda \rho}\frac{dI_\lambda}{ds} = I_\lambda - S_\lambda.} \tag{9.34}$$

This is one form of the **equation of radiative transfer** (usually referred to as the **transfer equation**).[24] According to the transfer equation, if the intensity of the light does not vary (so that the left-hand side of the equation is zero), then the intensity is equal to the source function, $I_\lambda = S_\lambda$. If the intensity of the light is *greater* than the source function (the right-hand side of the transfer equation is greater than 0), then $dI_\lambda/ds$ is less than 0, and the intensity *decreases* with distance. On the other hand, if the intensity is *less* than the source function, the intensity *increases* with distance. This is merely a mathematical restatement of the tendency of the photons found in the beam to resemble the local source of photons in the surrounding gas. Thus *the intensity of the light tends to become equal to the local value of the source function*, although the source function itself may vary too rapidly with distance for an equality to be attained.

### The Special Case of Blackbody Radiation

The source function for the special case of blackbody radiation can be found by considering a box of optically thick gas maintained at a constant temperature $T$. The confined particles and blackbody radiation are in thermodynamic equilibrium, with no net flow of energy through the box or between the gas particles and the radiation. With the particles and photons in equilibrium, individually and with each other, every process of absorption is balanced by an inverse process of emission. The intensity of the radiation is described by the Planck function, $I_\lambda = B_\lambda$. Furthermore, because the intensity is constant throughout the box, $dI_\lambda/ds = 0$, and so $I_\lambda = S_\lambda$. *For the case of thermodynamic equilibrium, the source function is equal to the Planck function*, $S_\lambda = B_\lambda$.

As mentioned in Section 9.2, a star cannot be in perfect thermodynamic equilibrium; there is a net flow of energy from the center to the surface. Deep in the atmosphere, where $\tau_\lambda \gg 1$ as measured along a vertical ray, a random-walking photon will take at least $\tau_\lambda^2$ steps to reach the surface (recall Eq. 9.30) and so will suffer many scattering events before escaping from the star. Thus, at a depth at which the photon mean free path is small compared to the

[23] As a ratio involving the inverse processes of absorption and emission, the source function is less sensitive to the detailed properties of the stellar material than are $j_\lambda$ and $\kappa_\lambda$ individually.

[24] It is assumed that the atmosphere is in a steady state, not changing with time. Otherwise, a time-derivative term would have to be included in the transfer equation.

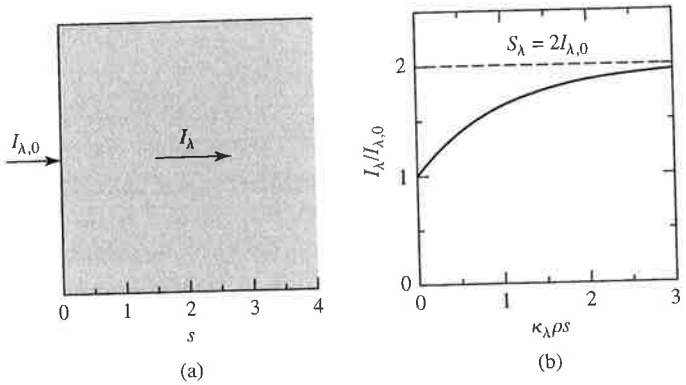


**FIGURE 9.13** Transformation of the intensity of a light ray traveling through a volume of gas. (a) A light ray entering a volume of gas. (b) Intensity of the light ray. The horizontal axis has units of $\kappa_\lambda \rho s$, the number of optical depths traveled into the gas.

temperature scale height, the photons are effectively confined to a limited volume, a region of nearly constant temperature. The conditions for local thermodynamic equilibrium (LTE) are satisfied, and so, as already seen, the source function is equal to the Planck function, $S_\lambda = B_\lambda$. Making the assumption of LTE in a problem means setting $S_\lambda = B_\lambda$. However, even in LTE, the intensity of the radiation, $I_\lambda$, will not necessarily be equal to $B_\lambda$ unless $\tau_\lambda \gg 1$. In summary, saying that $I_\lambda = B_\lambda$ is a statement that the radiation field is described by the Planck function, while $S_\lambda = B_\lambda$ describes the physical source of the radiation, $j_\lambda/\kappa_\lambda$, as one that produces blackbody radiation.

---

**Example 9.4.1.** To see how the intensity of a light ray tends to become equal to the local value of the source function, imagine a beam of light of initial intensity $I_{\lambda,0}$ at $s = 0$ entering a volume of gas of constant density, $\rho$, that has a *constant* opacity, $\kappa_\lambda$, and a *constant* source function, $S_\lambda$. Then it is left as an exercise to show that the transfer equation (Eq. 9.34) may be easily solved for the intensity of the light as a function of the distance $s$ traveled into the gas:

$$I_\lambda(s) = I_{\lambda,0}\, e^{-\kappa_\lambda \rho s} + S_\lambda(1 - e^{-\kappa_\lambda \rho s}). \tag{9.35}$$

As shown in Fig. 9.13 for the case of $S_\lambda = 2I_{\lambda,0}$, this solution describes the transformation of the intensity of the light ray from its initial value of $I_{\lambda,0}$ to $S_\lambda$, the value of the source function. The characteristic distance for this change to occur is $s = 1/\kappa_\lambda \rho$, which is one photon mean free path (recall Example 9.2.2), or one optical depth into the gas.

---

### The Assumption of a Plane-Parallel Atmosphere

Although the transfer equation is the basic tool that describes the passage of light through a star's atmosphere, a reader seeing it for the first time may be prone to despair. In this troublesome equation, the intensity of the light must depend on the direction of travel to account

for the net outward flow of energy. And although absorption and emission coefficients are the same for light traveling in all directions (implying that the source function is independent of direction), the absorption and emission coefficients depend on the temperature and density in a rather complicated way.

However, if astronomers are to learn anything about the physical conditions in stellar atmospheres, such as temperature or density, they must know where (at what depth) a spectral line is formed. A vast amount of effort has therefore been devoted to solving and understanding the implications of the transfer equation, and several powerful techniques have been developed that simplify the analysis considerably.

We will begin by rewriting Eq. (9.34) in terms of the optical depth $\tau_\lambda$, defined by Eq. (9.15), resulting in

$$\frac{dI_\lambda}{d\tau_\lambda} = I_\lambda - S_\lambda. \tag{9.36}$$

Unfortunately, because the optical depth is measured along the path of the light ray, neither the optical depth nor the distance $s$ in Eq. (9.34) corresponds to a unique geometric depth in the atmosphere. Consequently, the optical depth must be replaced by a meaningful measure of position.

To find a suitable replacement, we introduce the first of several standard approximations. The atmospheres of stars near the main sequence are physically thin compared with the size of the star, analogous to the skin of an onion. The atmosphere's radius of curvature is thus much larger than its thickness, and we may consider the atmosphere as a *plane-parallel slab*. As shown in Fig. 9.14, the $z$-axis is assumed to be in the vertical direction, with $z = 0$ at the top of this **plane-parallel atmosphere**.

Next, a **vertical optical depth**, $\tau_{\lambda,v}(z)$, is defined as

$$\tau_{\lambda,v}(z) \equiv \int_z^0 \kappa_\lambda \rho \, dz. \tag{9.37}$$

Comparison with Eq. (9.17) reveals that this is just the initial optical depth of a ray traveling

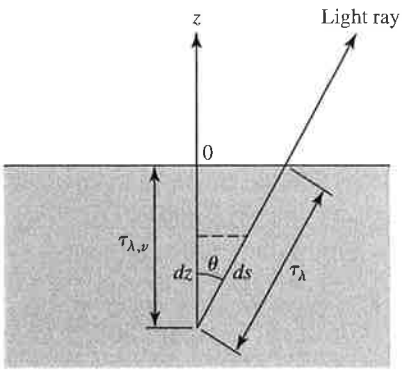


**FIGURE 9.14** Plane-parallel stellar atmosphere.

vertically upward from an initial position ($z < 0$) to the surface ($z = 0$) where $\tau_{\lambda,v} = 0$.[25] However, a ray that travels upward at an angle $\theta$ from the same initial position $z$ has farther to go through the same layers of the atmosphere in order to reach the surface. Therefore, the optical depth measured along this ray's path to the surface, $\tau_\lambda$, is *greater* than the vertical optical depth, $\tau_{\lambda,v}(z)$. Since $dz = ds\cos\theta$, the two optical depths are related by

$$\tau_\lambda = \frac{\tau_{\lambda,v}}{\cos\theta} = \tau_{\lambda,v}\sec\theta. \tag{9.38}$$

The vertical optical depth is a true vertical coordinate, analogous to $z$, that increases in the $-z$-direction. Its value does not depend on the direction of travel of a light ray, and so it can be used as a meaningful position coordinate in the transfer equation. Replacing $\tau_\lambda$ by $\tau_{\lambda,v}$ in Eq. (9.36) results in

$$\cos\theta\,\frac{dI_\lambda}{d\tau_{\lambda,v}} = I_\lambda - S_\lambda. \tag{9.39}$$

This form of the transfer equation is usually employed when dealing with the approximation of a plane-parallel atmosphere.

Of course, the value of the vertical optical depth at a level $z$ is wavelength-dependent because of the wavelength-dependent opacity in Eq. (9.37). In order to simplify the following analysis, and to permit the identification of an atmospheric level with a unique value of $\tau_v$, the opacity is assumed to be *independent of wavelength* (we usually take it to be equal to the Rosseland mean opacity, $\overline{\kappa}$). A model stellar atmosphere, for which the simplifying assumption is made that the opacity is independent of wavelength, is called a *gray atmosphere*, reflecting its indifference to the spectrum of wavelengths. If we write $\overline{\kappa}$ instead of $\kappa_\lambda$ in Eq. (9.37), the vertical optical depth no longer depends on wavelength; we can therefore write $\tau_v$ instead of $\tau_{\lambda,v}$ in the transfer equation (Eq. 9.39). The remaining wavelength dependencies may be removed by integrating the transfer equation over all wavelengths, using

$$I = \int_0^\infty I_\lambda\,d\lambda \qquad \text{and} \qquad S = \int_0^\infty S_\lambda\,d\lambda.$$

With the preceding changes, the transfer equation appropriate for a plane-parallel gray atmosphere is

$$\cos\theta\,\frac{dI}{d\tau_v} = I - S. \tag{9.40}$$

This equation leads to two particularly useful relations between the various quantities describing the radiation field. First, integrating over all solid angles, and recalling that $S$ depends only on the local conditions of the gas, independent of direction, we get

$$\frac{d}{d\tau_v}\int I\cos\theta\,d\Omega = \int I\,d\Omega - S\int d\Omega. \tag{9.41}$$

[25] Recall that as the light approaches the surface (and the observer on Earth), it is traveling through smaller and smaller values of the optical depth.

Using $\int d\Omega = 4\pi$ together with the definitions of the radiative flux $F_{\rm rad}$ (Eq. 9.8) and the mean intensity $\langle I \rangle$ (Eq. 9.3), both integrated over all wavelengths, we find

$$\frac{dF_{\rm rad}}{d\tau_v} = 4\pi(\langle I \rangle - S).$$

The second relation is found by first multiplying the transfer equation (9.40) by $\cos\theta$ and again integrating over all solid angles:

$$\frac{d}{d\tau_v}\int I\cos^2\theta\, d\Omega = \int I\cos\theta\, d\Omega - S\int \cos\theta\, d\Omega.$$

The term on the left is the radiation pressure multiplied by the speed of light (recall Eq. 9.9). The first term on the right-hand side is the radiative flux. In spherical coordinates, the second integral on the right-hand side evaluates to

$$\int \cos\theta\, d\Omega = \int_{\phi=0}^{2\pi}\int_{\theta=0}^{\pi} \cos\theta\sin\theta\, d\theta\, d\phi = 0.$$

Thus

$$\frac{dP_{\rm rad}}{d\tau_v} = \frac{1}{c}F_{\rm rad}. \tag{9.42}$$

In Problem 9.16, you will find that in a spherical coordinate system with its origin at the center of the star, this equation is

$$\frac{dP_{\rm rad}}{dr} = -\frac{\overline{\kappa}\rho}{c}F_{\rm rad},$$

which is just Eq. (9.31). As mentioned previously, this result can be interpreted as saying that the net radiative flux is driven by differences in the radiation pressure, with a "photon wind" blowing from high to low $P_{\rm rad}$. Equation (9.31) will be employed in Chapter 10 to determine the temperature structure in the interior of a star.

In an equilibrium stellar atmosphere, every process of absorption is balanced by an inverse process of emission; no net energy is subtracted from or added to the radiation field. In a plane-parallel atmosphere, this means that the radiative flux must have the same value at every level of the atmosphere, including its surface. From Eq. (3.18),

$$F_{\rm rad} = \text{constant} = F_{\rm surf} = \sigma T_e^4. \tag{9.43}$$

Because the flux is a constant, $dF_{\rm rad}/d\tau_v = 0$, so Eq. (9.4) implies that the mean intensity must be equal to the source function,

$$\langle I \rangle = S. \tag{9.44}$$

Equation (9.42) may now be integrated to find the radiation pressure as a function of the vertical optical depth:

$$P_{\rm rad} = \frac{1}{c}F_{\rm rad}\tau_v + C, \tag{9.45}$$

where $C$ is the constant of integration.

### The Eddington Approximation

If we knew how the radiation pressure varied with temperature for the general case (and not just for blackbody radiation), we could use Eq. (9.45) to determine the temperature structure of our plane-parallel gray atmosphere. We would have to *assume* a description of the angular distribution of the intensity. In an approximation that we owe to the brilliant English physicist Sir Arthur Stanley Eddington (1882–1944), the intensity of the radiation field is assigned one value, $I_{\text{out}}$, in the $+z$-direction (outward) and another value, $I_{\text{in}}$, in the $-z$-direction (inward); see Fig. 9.15. Both $I_{\text{out}}$ and $I_{\text{in}}$ vary with depth in the atmosphere, and in particular, $I_{\text{in}} = 0$ at the top of the atmosphere, where $\tau_\nu = 0$. It is left as an exercise to show that with this **Eddington approximation**,[26] the mean intensity, radiative flux, and radiation pressure are given by

$$\langle I \rangle = \frac{1}{2}\,(I_{\text{out}} + I_{\text{in}}) \tag{9.46}$$

$$F_{\text{rad}} = \pi\,(I_{\text{out}} - I_{\text{in}}) \tag{9.47}$$

$$P_{\text{rad}} = \frac{2\pi}{3c}\,(I_{\text{out}} + I_{\text{in}}) = \frac{4\pi}{3c}\,\langle I \rangle. \tag{9.48}$$

[Note that because the flux is a constant, Eq. (9.47) shows that there is a constant difference between $I_{\text{out}}$ and $I_{\text{in}}$ at any level of the atmosphere.]

Inserting the last relation for the radiation pressure into Eq. (9.45), we find that

$$\frac{4\pi}{3c}\,\langle I \rangle = \frac{1}{c}\,F_{\text{rad}}\tau_\nu + C. \tag{9.49}$$

The constant $C$ can be determined by evaluating Eqs. (9.46) and (9.47) at the top of the atmosphere, where $\tau_\nu = 0$ and $I_{\text{in}} = 0$. The result is that $\langle I\,(\tau_\nu = 0) \rangle = F_{\text{rad}}/2\pi$. Inserting

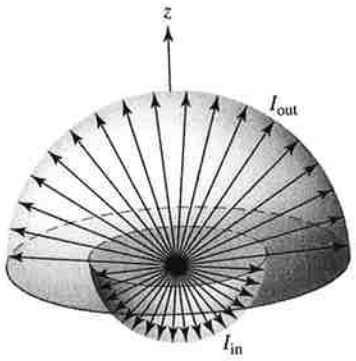


**FIGURE 9.15** The Eddington approximation.

[26] Actually, there are several more mathematical ways of implementing the Eddington approximation, but they are all equivalent.

this into Eq. (9.49) with $\tau_v = 0$ shows that

$$C = \frac{2}{3c} F_{\text{rad}}.$$

With this value of $C$, Eq. (9.49) becomes

$$\frac{4\pi}{3} \langle I \rangle = F_{\text{rad}} \left( \tau_v + \frac{2}{3} \right). \tag{9.50}$$

Of course, we already know that the radiative flux is a constant, given by Eq. (9.43). Using this results in an expression for the mean intensity as a function of the vertical optical depth:

$$\langle I \rangle = \frac{3\sigma}{4\pi} T_e^4 \left( \tau_v + \frac{2}{3} \right). \tag{9.51}$$

We may now derive the final approximation to determine the temperature structure of our model atmosphere. If the atmosphere is assumed to be in local thermodynamic equilibrium, another expression for the mean intensity can be found and combined with Eq. (9.51). By the definition of LTE, the source function is equal to the Planck function, $S_\lambda = B_\lambda$. Integrating $B_\lambda$ over all wavelengths (see Eq. 3.28) shows that for LTE,

$$S = B = \frac{\sigma T^4}{\pi},$$

and so, from Eq. (9.44),

$$\langle I \rangle = \frac{\sigma T^4}{\pi}. \tag{9.52}$$

Equating expressions (9.51) and (9.52) finally results in the variation of the temperature with vertical optical depth in a plane-parallel gray atmosphere in LTE, assuming the Eddington approximation:[27]

$$\boxed{T^4 = \frac{3}{4} T_e^4 \left( \tau_v + \frac{2}{3} \right).} \tag{9.53}$$

This relation is well worth the effort of its derivation, because it reveals some important aspects of real stellar atmospheres. First, notice that $T = T_e$ at $\tau_v = 2/3$, *not* at $\tau_v = 0$. Thus the "surface" of a star, which by definition has temperature $T_e$ [recall the Stefan–Boltzmann equation, Eq. (3.17)], is *not* at the top of the atmosphere, where $\tau_v = 0$, but deeper down, where $\tau_v = 2/3$. This result may be thought of as the average point of origin of the observed photons. Although this result came at the end of a string of assumptions, it can be generalized to the statement that *when looking at a star, we see down to a vertical optical depth of* $\tau_v \approx 2/3$, *averaged over the disk of the star*. The importance of this for the formation and interpretation of spectral lines was discussed on page 254.

[27] You are encouraged to refer to Mihalas, Chapter 3, for a more detailed discussion of the gray atmosphere, including a more sophisticated development of the relation $T^4 = \frac{3}{4} T_e^4 \, [\tau_v + q(\tau_v)]$, where the Eddington approximation $[q(\tau_v) \equiv \frac{2}{3}]$ is a special case.

## Limb Darkening Revisited

We now move on to take a closer look at limb darkening (recall Fig. 9.12). A comparison of theory and observations of limb darkening can provide valuable information about how the source function varies with depth in a star's atmosphere. To see how this is done, we first solve the general form of the transfer equation (Eq. 9.36),

$$\frac{dI_\lambda}{d\tau_\lambda} = I_\lambda - S_\lambda,$$

at least formally, rather than by making assumptions. (The inevitable assumptions will be required soon enough.) Multiplying both sides by $e^{-\tau_\lambda}$, we have

$$\frac{dI_\lambda}{d\tau_\lambda} e^{-\tau_\lambda} - I_\lambda e^{-\tau_\lambda} = -S_\lambda e^{-\tau_\lambda}$$

$$\frac{d}{d\tau_\lambda}(e^{-\tau_\lambda} I_\lambda) = -S_\lambda e^{-\tau_\lambda}$$

$$d(e^{-\tau_\lambda} I_\lambda) = -S_\lambda e^{-\tau_\lambda} d\tau_\lambda.$$

If we integrate from the initial position of the ray, at optical depth $\tau_{\lambda,0}$ where $I_\lambda = I_{\lambda,0}$, to the top of the atmosphere, at optical depth $\tau_\lambda = 0$ where $I_\lambda = I_\lambda(0)$, the result for the emergent intensity at the top of the atmosphere, $I_\lambda(0)$, is

$$I_\lambda(0) = I_{\lambda,0} e^{-\tau_{\lambda,0}} - \int_{\tau_{\lambda,0}}^{0} S_\lambda e^{-\tau_\lambda} d\tau_\lambda. \tag{9.54}$$

This equation has a very straightforward interpretation. The emergent intensity on the left is the sum of two positive contributions. The first term on the right is the initial intensity of the ray, reduced by the effects of absorption along the path to the surface. The second term, also positive,[28] represents the emission at every point along the path, attenuated by the absorption between the point of emission and the surface.

We now return to the geometry of a plane-parallel atmosphere and the vertical optical depth, $\tau_v$. However, we do *not* assume a gray atmosphere, LTE, or make the Eddington approximation. As shown in Fig. 9.16, the problem of limb darkening amounts to determining the emergent intensity $I_\lambda(0)$ as a function of the angle $\theta$. Equation (9.54), the formal solution to the transfer equation, is easily converted to this situation by using Eq. (9.38) to replace $\tau_\lambda$ with $\tau_{\lambda,v} \sec\theta$ (the vertical optical depth) to get

$$I(0) = I_0 e^{-\tau_{v,0} \sec\theta} - \int_{\tau_{v,0} \sec\theta}^{0} S \sec\theta \, e^{-\tau_v \sec\theta} \, d\tau_v.$$

Although both $I$ and $\tau_v$ depend on wavelength, the $\lambda$ subscript has been dropped to simplify the notation; the approximation of a gray atmosphere has *not* been made. To include the contributions to the emergent intensity from all layers of the atmosphere, we take the value

[28] Remember that the optical depth, measured along the ray's path, decreases in the direction of travel, so $d\tau_\lambda$ is negative.

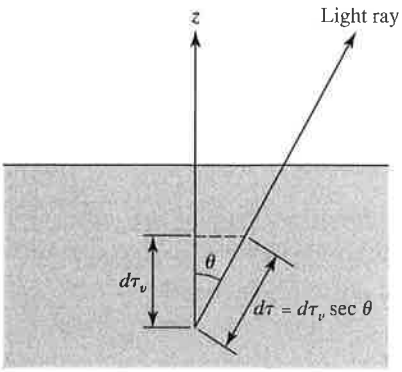


**FIGURE 9.16** Finding $I(0)$ as a function of $\theta$ for limb darkening in plane-parallel geometry.

of the initial position of the rays to be at $\tau_{v,0} = \infty$. Then the first term on the right-hand side vanishes, leaving

$$I(0) = \int_0^\infty S \sec\theta \, e^{-\tau_v \sec\theta} \, d\tau_v. \tag{9.55}$$

If we knew how the source function depends on the vertical optical depth, this equation could be integrated to find the emergent intensity as a function of the direction of travel, $\theta$, of the ray. Although the form of the source function is not known, a good guess will be enough to estimate $I(0)$. Suppose that the source function has the form

$$S = a + b\tau_v, \tag{9.56}$$

where $a$ and $b$ are wavelength-dependent numbers to be determined. Inserting this into Eq. (9.55) and integrating (the details are left as an exercise) show that the emergent intensity for this source function is

$$I_\lambda(0) = a_\lambda + b_\lambda \cos\theta, \tag{9.57}$$

where the $\lambda$ subscripts have been restored to the appropriate quantities to emphasize their wavelength dependence. By making careful measurements of the variation in the specific intensity across the disk of the Sun, the values of $a_\lambda$ and $b_\lambda$ for the solar source function can be determined for a range of wavelengths. For example, for a wavelength of 501 nm, Böhm-Vitense (1989) supplies values of $a_{501} = 1.04 \times 10^{13}$ W m$^{-3}$ sr$^{-1}$ and $b_{501} = 3.52 \times 10^{13}$ W m$^{-3}$ sr$^{-1}$.

---

**Example 9.4.2.** Solar limb darkening provides an opportunity to test the accuracy of our "plane-parallel gray atmosphere in LTE using the Eddington approximation." In the preceding discussion of an equilibrium gray atmosphere, it was found that the mean intensity is equal to the source function,

$$\langle I \rangle = S$$

*continued*

(Eq. 9.44). Then, with the additional assumptions of the Eddington approximation and LTE, Eqs. (9.52) and (9.53) can be used to determine the mean intensity and thus the source function:

$$S = \langle I \rangle = \frac{\sigma T^4}{\pi} = \frac{3\sigma}{4\pi} T_e^4 \left( \tau_v + \frac{2}{3} \right).$$

Taking the source function to have the form of Eq. (9.56), $S = a + b\tau_v$, as used earlier for limb darkening (*after integrating over all wavelengths*), the values of the coefficients are

$$a = \frac{\sigma}{2\pi} T_e^4 \qquad \text{and} \qquad b = \frac{3\sigma}{4\pi} T_e^4.$$

The emergent intensity then will have the form of Eq. (9.57), $I(0) = a + b\cos\theta$ (again after integrating over all wavelengths). The ratio of the emergent intensity at angle $\theta$, $I(\theta)$, to that at the center of the star, $I(\theta = 0)$, is thus

$$\frac{I(\theta)}{I(\theta = 0)} = \frac{a + b\cos\theta}{a + b} = \frac{2}{5} + \frac{3}{5}\cos\theta. \tag{9.58}$$

We can compare the results of this calculation with observations of solar limb darkening in integrated light (made by summing over all wavelengths). Figure 9.17 shows both the observed values of $I(\theta)/I(\theta = 0)$ and the values from Eq. (9.58). The agreement is remarkably good, despite our numerous approximations. However, be forewarned that the agreement is much worse for observations made at a given wavelength (see Böhm-Vitense, 1989) as a consequence of wavelength-dependent opacity effects such as line blanketing.

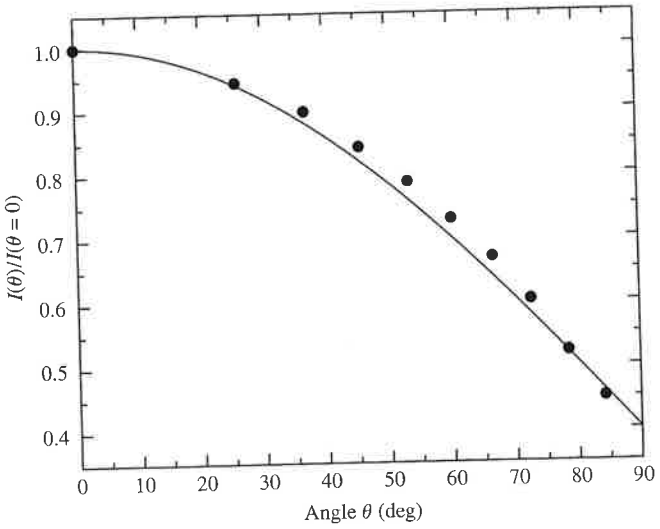


**FIGURE 9.17** A theoretical Eddington approximation of solar limb darkening for light integrated over all wavelengths. The dots are observational data for the Sun. Although a good fit, the Eddington approximation is not perfect, which implies that a more detailed model must be developed; see, for example, Problem 9.29.

## 9.5 ■ THE PROFILES OF SPECTRAL LINES

We now have a formidable theoretical arsenal to bring to bear on the analysis of spectral lines. The shape of an individual spectral line contains a wealth of information about the environment in which it was formed.

### Equivalent Widths

Figure 9.18 shows a graph of the radiant flux, $F_\lambda$, as a function of wavelength for a typical absorption line. In the figure, $F_\lambda$ is expressed as a fraction of $F_c$, the value of the flux from the continuous spectrum outside the spectral line. Near the central wavelength, $\lambda_0$, is the *core* of the line, and the sides sweeping upward to the continuum are the line's *wings*. Individual lines may be narrow or broad, shallow or deep. The quantity $(F_c - F_\lambda)/F_c$ is referred to as the *depth* of the line. The strength of a spectral line is measured in terms of its **equivalent width**. The equivalent width $W$ of a spectral line is defined as the width of a box (shaded in Fig. 9.18) reaching up to the continuum that has the same area as the spectral line. That is,

$$W = \int \frac{F_c - F_\lambda}{F_c}\, d\lambda, \tag{9.59}$$

where the integral is taken from one side of the line to the other. The equivalent width of a line in the visible spectrum, shaded in Fig. 9.18, is usually on the order of 0.01 nm. Another measure of the width of a spectral line is the change in wavelength from one side of the line to the other, where its depth $(F_c - F_\lambda)/(F_c - F_{\lambda_0}) = 1/2$; this is called the *full width at half-maximum* and will be denoted by $(\Delta\lambda)_{1/2}$.

The spectral line shown in Fig. 9.18 is termed **optically thin** because there is no wavelength at which the radiant flux has been completely blocked. The opacity $\kappa_\lambda$ of the stellar

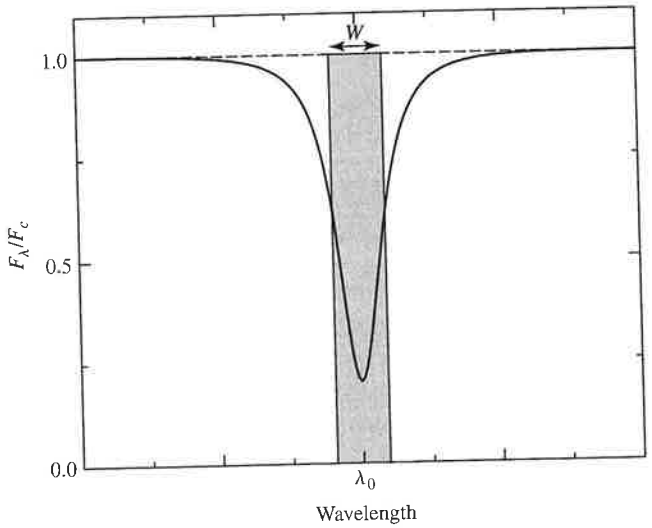


**FIGURE 9.18** The profile of a typical spectral line.

material is greatest at the wavelength $\lambda_0$ at the line's center and decreases moving into the wings. From the discussion on page 254, this means that the center of the line is formed at higher (and cooler) regions of the stellar atmosphere. Moving into the wings from $\lambda_0$, the line formation occurs at progressively deeper (and hotter) layers of the atmosphere, until it merges with the continuum-producing region at an optical depth of 2/3. In Section 11.2 this idea will be applied to the absorption lines produced in the solar photosphere.

### Processes That Broaden Spectral Lines

Three main processes are responsible for the broadening of spectral lines. Each of these mechanisms produces its own distinctive line shape or *line profile*.

1. **Natural broadening.** Spectral lines cannot be infinitely sharp, even for motionless, isolated atoms. According to Heisenberg's uncertainty principle (recall Eq. 5.20), as the time available for an energy measurement decreases, the inherent uncertainty of the result increases. Because an electron in an excited state occupies its orbital for only a brief instant, $\Delta t$, the orbital's energy, $E$, cannot have a precise value. Thus the uncertainty in the energy, $\Delta E$, of the orbital is approximately

$$\Delta E \approx \frac{\hbar}{\Delta t}.$$

(The electron's lifetime in the ground state may be taken as infinite, so in that case $\Delta E = 0$.) Electrons can make transitions from and to anywhere within these "fuzzy" energy levels, producing an uncertainty in the wavelength of the photon absorbed or emitted in a transition. Using Eq. (5.3) for the energy of a photon, $E_{\text{photon}} = hc/\lambda$, we find that the uncertainty in the photon's wavelength has a magnitude of roughly

$$\Delta\lambda \approx \frac{\lambda^2}{2\pi c}\left(\frac{1}{\Delta t_i} + \frac{1}{\Delta t_f}\right), \tag{9.60}$$

where $\Delta t_i$ is the lifetime of the electron in its initial state and $\Delta t_f$ is the lifetime in the final state. (The proof is left as a problem.)

---

**Example 9.5.1.** The lifetime of an electron in the first and second excited states of hydrogen is about $\Delta t = 10^{-8}$ s. The natural broadening of the H$\alpha$ line of hydrogen, $\lambda = 656.3$ nm, is then

$$\Delta\lambda \approx 4.57 \times 10^{-14}\ \text{m} = 4.57 \times 10^{-5}\ \text{nm}.$$

---

A more involved calculation shows that the full width at half-maximum of the line profile for natural broadening is

$$(\Delta\lambda)_{1/2} = \frac{\lambda^2}{\pi c}\frac{1}{\Delta t_0}, \tag{9.61}$$

where $\Delta t_0$ is the average waiting time for a specific transition to occur. This results in a typical value of

$$(\Delta\lambda)_{1/2} \simeq 2.4 \times 10^{-5} \text{ nm},$$

in good agreement with the preceding estimate.

2. **Doppler broadening.** In thermal equilibrium, the atoms in a gas, each of mass $m$, are moving randomly about with a distribution of speeds that is described by the Maxwell–Boltzmann distribution function (Eq. 8.1), with the most probable speed given by Eq. (8.2), $v_{\text{mp}} = \sqrt{2kT/m}$. The wavelengths of the light absorbed or emitted by the atoms in the gas are Doppler-shifted according to (nonrelativistic) Eq. (4.30), $\Delta\lambda/\lambda = \pm|v_r|/c$. Thus the width of a spectral line due to Doppler broadening should be approximately

$$\Delta\lambda \approx \frac{2\lambda}{c}\sqrt{\frac{2kT}{m}}.$$

---

**Example 9.5.2.** For hydrogen atoms in the Sun's photosphere ($T = 5777$ K), the Doppler broadening of the H$\alpha$ line should be about

$$\Delta\lambda \approx 0.0427 \text{ nm},$$

roughly 1000 times greater than for natural broadening.

---

A more in-depth analysis, taking into account the different directions of the atoms' motions with respect to one another and to the line of sight of the observer, shows that the full width at half-maximum of the line profile for Doppler broadening is

$$(\Delta\lambda)_{1/2} = \frac{2\lambda}{c}\sqrt{\frac{2kT\ln 2}{m}}. \tag{9.62}$$

Although the line profile for Doppler broadening is much wider at half-maximum than for natural broadening, the line depth for Doppler broadening decreases *exponentially* as the wavelength moves away from the central wavelength $\lambda_0$. This rapid decline is due to the high-speed exponential "tail" of the Maxwell–Boltzmann velocity distribution and is a much faster falloff in strength than for natural broadening.

Doppler shifts caused by the large-scale turbulent motion of large masses of gas (as opposed to the random motion of the individual atoms) can also be accommodated by Eq. (9.62) if the distribution of turbulent velocities follows the Maxwell–Boltzmann distribution. In that case,

$$(\Delta\lambda)_{1/2} = \frac{2\lambda}{c}\sqrt{\left(\frac{2kT}{m} + v_{\text{turb}}^2\right)\ln 2}, \tag{9.63}$$

where $v_{\text{turb}}$ is the most probable turbulent speed. The effect of turbulence on line profiles is particularly important in the atmospheres of giant and supergiant stars. In

fact, the existence of turbulence in the atmospheres of these stars was first deduced from the inordinately large effect of Doppler broadening on their spectra.

Other sources of Doppler broadening involve orderly, coherent mass motions, such as stellar rotation, pulsation, and mass loss. These phenomena can have a substantial effect on the shape and width of the line profiles but cannot be combined with the results of Doppler broadening produced by random thermal motions obeying the Maxwell–Boltzmann distribution. For example, the characteristic P Cygni profile associated with mass loss will be discussed in Section 12.3 (see Fig. 12.17).

3. **Pressure (and collisional) broadening.** The orbitals of an atom can be perturbed in a collision with a neutral atom or by a close encounter involving the electric field of an ion. The results of individual collisions are called *collisional broadening*, and the statistical effects of the electric fields of large numbers of closely passing ions is termed *pressure broadening*; however, in the following discussion, both of these effects will be collectively referred to as pressure broadening. In either case, the outcome depends on the average time between collisions or encounters with other atoms and ions.

Calculating the precise width and shape of a pressure-broadened line is quite complicated. Atoms and ions of the same or different elements, as well as free electrons, are involved in these collisions and close encounters. The general shape of the line, however, is like that found for natural broadening, Eq. (9.61), and the line profile shared by natural and pressure broadening is sometimes referred to as a *damping profile* (also known as a *Lorentz profile*), so named because the shape is characteristic of the spectrum of radiation emitted by an electric charge undergoing damped simple harmonic motion. The values of the full width at half-maximum for natural and pressure broadening usually prove to be comparable, although the pressure profile can at times be more than an order of magnitude wider.

An estimate of pressure broadening due to collisions with atoms of a single element can be obtained by taking the value of $\Delta t_0$ in Eq. (9.61) to be the average time between collisions. This time is approximately equal to the mean free path between collisions divided by the average speed of the atoms. Using Eq. (9.12) for the mean free path and Eq. (8.2) for the speed, we find that

$$\Delta t_0 \approx \frac{\ell}{v} = \frac{1}{n\sigma\sqrt{2kT/m}},$$

where $m$ is the mass of an atom, $\sigma$ is its collision cross section, and $n$ is the number density of the atoms. Thus the width of the spectral line due to pressure broadening is on the order of

$$\Delta\lambda = \frac{\lambda^2}{c}\frac{1}{\pi\Delta t_0} \approx \frac{\lambda^2}{c}\frac{n\sigma}{\pi}\sqrt{\frac{2kT}{m}}. \tag{9.64}$$

Note that the width of the line is proportional to the number density $n$ of the atoms.

The physical reason for the Morgan–Keenan luminosity classes is now clear. The narrower lines observed for the more luminous giant and supergiant stars are due to

the lower number densities in their extended atmospheres. Pressure broadening (with the width of the line profile proportional to $n$) broadens the lines formed in the denser atmospheres of main-sequence stars, where collisions occur more frequently.

**Example 9.5.3.** Again, consider the hydrogen atoms in the Sun's photosphere, where the temperature is 5777 K and the number density of hydrogen atoms is about $1.5 \times 10^{23}$ m$^{-3}$. Then the pressure broadening of the H$\alpha$ line should be roughly

$$\Delta\lambda \approx 2.36 \times 10^{-5} \text{ nm},$$

which is comparable to the result for natural broadening found earlier. However, if the number density of the atoms in the atmosphere of a star is larger, the line width will be larger as well—more than an order of magnitude larger in some cases.

### The Voigt Profile

The total line profile, called a **Voigt profile**, is due to the contributions of both the Doppler and damping profiles. The wider line profile for Doppler broadening dominates near the central wavelength $\lambda_0$. Farther from $\lambda_0$, however, the exponential decrease in the line depth for Doppler broadening means that there is a transition to a damping profile in the wings at a distance of about 1.8 times the Doppler value of $(\Delta\lambda)_{1/2}$ from the center of the line. Thus line profiles tend to have *Doppler cores* and *damping wings*. Figure 9.19 schematically shows the Doppler and damping line profiles.

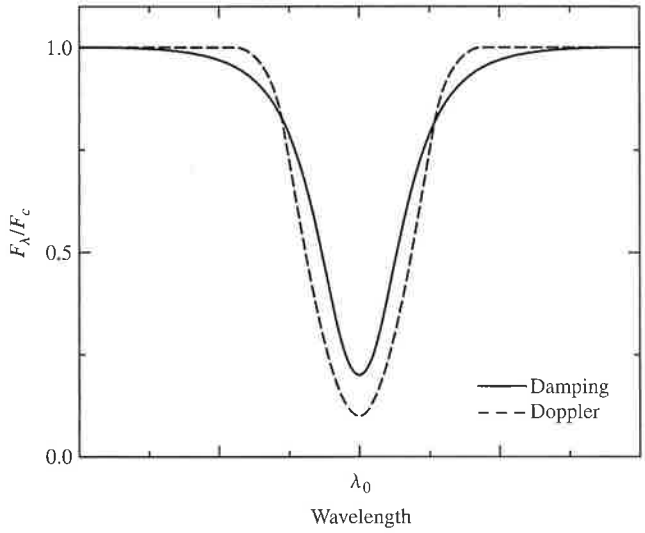


**FIGURE 9.19** Schematic damping and Doppler line profiles, scaled so they have the same equivalent width.

**Example 9.5.4.** As a review of the ideas of spectral line formation discussed here and in Chapter 8, consider the subdwarfs of luminosity class VI or "sd," which reside to the left of the main sequence (see Fig. 8.16). The spectra of these subdwarfs show that they are deficient in the atoms of metals (elements heavier than helium). Because ionized metals are an important source of electrons in stellar atmospheres, the electron number density is reduced. As mentioned in Section 8.1, fewer electrons with which ions may recombine means that a higher degree of ionization for all atoms can be achieved at the same temperature. Specifically, this reduces the number of $H^-$ ions in the atmosphere by ionizing them, thereby diluting this dominant source of continuum opacity. As a consequence of a lower opacity, we can see longer distances into these stars before reaching an optical depth of $\tau_\lambda = 2/3$. The forest of metallic lines (which are already weakened by the low metal abundance of the subdwarfs) appears even weaker against the brighter continuum. Thus, as a result of an under-abundance of metals, the spectrum of a subdwarf appears to be that of a hotter and brighter star of earlier spectral type with less prominent metal lines (see Table 8.1). This is why it is more accurate to say that these stars are displaced to the *left* of the main sequence, toward higher temperatures, rather than one magnitude below the main sequence.

The simplest model used for calculating a line profile assumes that the star's photosphere acts as a source of blackbody radiation and that the atoms above the photosphere remove photons from this continuous spectrum to form absorption lines. Although this **Schuster–Schwarzschild model** is inconsistent with the idea that photons of wavelength $\lambda$ originate at an optical depth of $\tau_\lambda = 2/3$, it is still a useful approximation. In order to carry out the calculation, values for the temperature, density, and composition must be adopted for the region above the photosphere where the line is formed. The temperature and density determine the importance of Doppler and pressure broadening and are also used in the Boltzmann and Saha equations.

The calculation of a spectral line depends not only on the abundance of the element forming the line but also on the quantum-mechanical details of how atoms absorb photons. Let $N$ be the number of atoms of a certain element lying *above a unit area* of the photosphere. $N$ is a **column density** and has units of $m^{-2}$. (In other words, suppose a hollow tube with a cross section of 1 $m^2$ was stretched from the observer to the photosphere; the tube would then contain $N$ atoms of the specified type.) To find the number of absorbing atoms per unit area, $N_a$, that have electrons in the proper orbital for absorbing a photon at the wavelength of the spectral line, the temperature and density are used in the Boltzmann and Saha equations to calculate the atomic states of excitation and ionization. Our goal is to determine the value of $N_a$ by comparing the calculated and observed line profiles.

This task is complicated by the fact that not all transitions between atomic orbitals are equally likely. For example, an electron initially in the $n = 2$ orbital of hydrogen is about five times more likely to absorb an H$\alpha$ photon and make a transition to the $n = 3$ orbital than it is to absorb an H$\beta$ photon and jump to the $n = 4$ orbital. The relative probabilities of an electron making a transition from the same initial orbital are given by the *f-values* or *oscillator strengths* for that orbital. For hydrogen, $f = 0.637$ for the H$\alpha$ transition and $f = 0.119$ for H$\beta$. The oscillator strengths may be calculated numerically or measured in the laboratory, and they are defined so that the $f$-values for transitions from the same initial

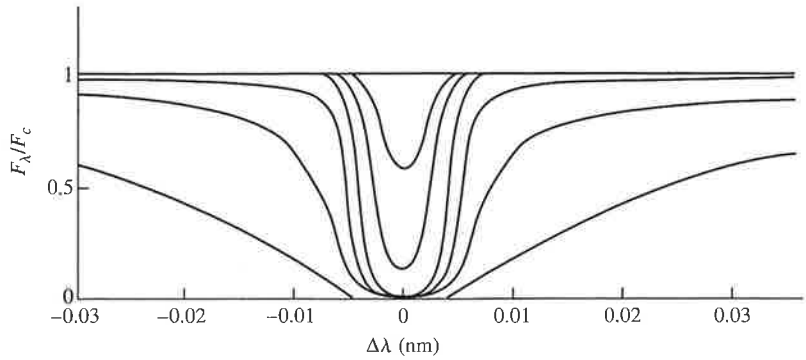


**FIGURE 9.20** Voigt profiles of the K line of Ca II. The shallowest line is produced by $N_a = 3.4 \times 10^{15}$ ions $m^{-2}$, and the ions are ten times more abundant for each successively broader line. (Adapted from Novotny, *Introduction to Stellar Atmospheres and Interiors*, Oxford University Press, New York, 1973.)

orbital add up to the number of electrons in the atom or ion. Thus the oscillator strength is the effective number of electrons per atom participating in a transition, and so multiplying the number of absorbing atoms per unit area by the $f$-value gives the number of atoms lying above each square meter of the photosphere that are actively involved in producing a given spectral line, $fN_a$. Figure 9.20 shows the Voigt profiles of the K line of Ca II ($\lambda = 393.3$ nm) for various values of the number of absorbing calcium ions.

## The Curve of Growth

The **curve of growth** is an important tool that astronomers use to determine the value of $N_a$ and thus the abundances of elements in stellar atmospheres. As seen in Fig. 9.20, the equivalent width, $W$, of the line varies with $N_a$. A curve of growth, shown in Fig. 9.21, is a logarithmic graph of the equivalent width, $W$, as a function of the number of absorbing atoms, $N_a$. To begin with, imagine that a specific element is not present in a stellar atmosphere. As some of that element is introduced, a weak absorption line appears that is initially optically thin. If the number of the absorbing atoms is doubled, twice as much light is removed, and the equivalent width of the line is twice as great. So $W \propto N_a$, and the curve of growth is initially linear with $\ln N_a$. As the number of absorbing atoms continues to increase, the center of the line becomes optically thick as the maximum amount of flux at the line's center is absorbed.[29] With the addition of still more atoms, the line bottoms out and becomes saturated. The wings of the line, which are still optically thin, continue to deepen. This occurs with relatively little change in the line's equivalent width and produces a flattening on the curve of growth where $W \propto \sqrt{\ln N_a}$. Increasing the number of absorbing atoms still further increases the width of the pressure-broadening profile [recall Eq. (9.64)],

[29]The zero flux at the center of the line shown in Fig. 9.20 is a peculiarity of the Schuster–Schwarzschild model. Actually, there is always *some* flux received at the central wavelength, $\lambda_0$, even for very strong, optically thick lines. As a rule, the flux at any wavelength cannot fall below $F_\lambda = \pi S_\lambda(\tau_\lambda = 2/3)$, the value of the source function at an optical depth of 2/3; see Problem 9.20.

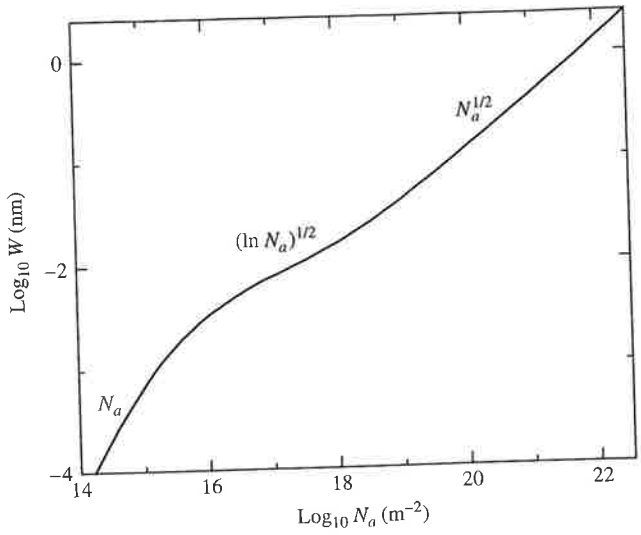


**FIGURE 9.21** The curve of growth for the K line of Ca II. As $N_a$ increases, the functional dependence of the equivalent width ($W$) changes. At various positions along the curve of growth, $W$ is proportional to the functional forms indicated. (Figure adapted from Aller, *The Atmospheres of the Sun and Stars*, Ronald Press, New York, 1963.)

enabling it to contribute to the wings of the line. The equivalent width grows more rapidly, although not as steeply as at first, with approximately $W \propto \sqrt{N_a}$ for the total line profile. Using the curve of growth and a measured equivalent width, we can obtain the number of absorbing atoms. The Boltzmann and Saha equations are then used to convert this value into the total number of atoms of that element lying above the photosphere.

To reduce the errors involved in using a single spectral line, it is advantageous to locate, on a single curve of growth, the positions of the equivalent widths of several lines formed by transitions from the same initial orbital.[30] This can be accomplished by plotting $\log_{10}(W/\lambda)$ on the vertical axis and $\log_{10}[f N_a(\lambda/500\ \text{nm})]$ on the horizontal axis. This scaling results in a general curve of growth that can be used for several lines. Figure 9.22 shows a general curve of growth for the Sun. The use of such a curve of growth is best illustrated by an example.

---

**Example 9.5.5.** We will use Fig. 9.22 to find the number of sodium atoms above each square meter of the Sun's photosphere from measurements of the 330.238-nm and 588.997-nm absorption lines of sodium (Table 9.1). Values of $T = 5800$ K and $P_e = 1\ \text{N m}^{-2}$ were used for the temperature and electron pressure, respectively, to construct this curve of growth and will be adopted in the calculations that follow.

Both of these lines are produced when an electron makes an upward transition from the ground state orbital of the neutral Na I atom, and so these lines have the same value of $N_a$,

[30] This is just one of several possible ways of scaling the curve of growth. The assumptions used to obtain such a scaling are not valid for all broad lines (such as hydrogen) and may lead to inaccurate results.

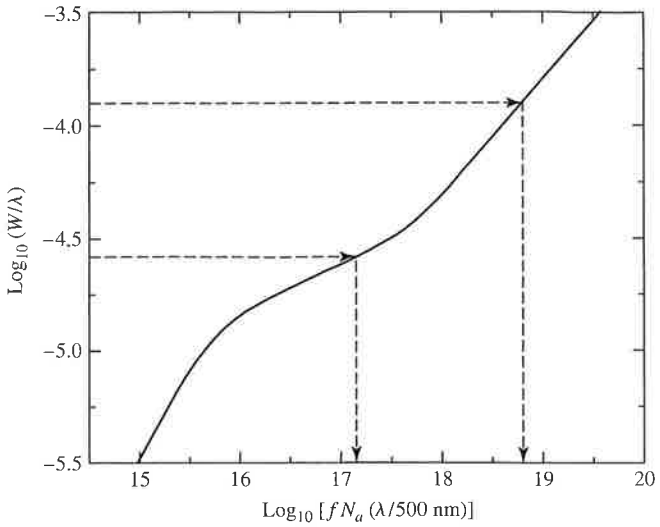


**FIGURE 9.22** A general curve of growth for the Sun. The arrows refer to the data used in Example 9.5.5. (Figure adapted from Aller, *Atoms, Stars, and Nebulae*, Revised Edition, Harvard University Press, Cambridge, MA, 1971.)

**TABLE 9.1** Data for Solar Sodium Lines. (From Aller, *Atoms, Stars, and Nebulae*, Revised Edition, Harvard University Press, Cambridge, MA, 1971.)

| $\lambda$ (nm) | $W$ (nm) | $f$ | $\log_{10}(W/\lambda)$ | $\log_{10}[f(\lambda/500\text{ nm})]$ |
|---|---|---|---|---|
| 330.238 | 0.0088 | 0.0214 | −4.58 | −1.85 |
| 588.997 | 0.0730 | 0.645 | −3.90 | −0.12 |

the number of absorbing sodium atoms per unit area above the continuum-forming layer of the photosphere. This number can be found using the values of $\log_{10}(W/\lambda)$ with the general curve of growth, Fig. 9.22, to obtain a value of $\log_{10}[fN_a(\lambda/500\text{ nm})]$ for each line. The results are

$$\log_{10}\left(\frac{fN_a\lambda}{500\text{ nm}}\right) = 17.20 \quad \text{for the 330.238 nm line}$$

$$= 18.83 \quad \text{for the 588.997 nm line.}$$

To obtain the value of the number of absorbing atoms per unit area, $N_a$, we use the measured values of $\log_{10}[f(\lambda/500\text{ nm})]$ together with

$$\log_{10} N_a = \log_{10}\left(\frac{fN_a\lambda}{500\text{ nm}}\right) - \log_{10}\left(\frac{f\lambda}{500\text{ nm}}\right),$$

to find

$$\log_{10} N_a = 17.15 - (-1.85) = 19.00 \quad \text{for the 330.238 nm line}$$

*continued*

and

$$\log_{10} N_a = 18.80 - (-0.12) = 18.92 \quad \text{for the 588.997 nm line.}$$

The average value of $\log_{10} N_a$ is 18.96; thus there are about $10^{19}$ Na I atoms in the ground state per square meter of the photosphere.

To find the total number of sodium atoms, the Boltzmann and Saha equations must be used; Eqs. (8.6) and (8.9), respectively. The difference in energy between the final and initial states [$E_b - E_a$ in Eq. (8.6)] is just the energy of the emitted photon. Using Eq. (5.3), the exponential term in the Boltzmann equation is

$$\begin{aligned} e^{-(E_b - E_a)/kT} &= e^{-hc/\lambda kT} \\ &= 5.45 \times 10^{-4} \quad \text{for the 330.238 nm line} \\ &= 1.48 \times 10^{-2} \quad \text{for the 588.997 nm line,} \end{aligned}$$

so nearly all of the neutral Na I atoms are in the ground state.

All that remains is to determine the total number of sodium atoms per unit area in all stages of ionization. If there are $N_{\mathrm{I}} = 10^{19}$ neutral sodium atoms per square meter, then the number of singly ionized atoms, $N_{\mathrm{II}}$, comes from the Saha equation:

$$\frac{N_{\mathrm{II}}}{N_{\mathrm{I}}} = \frac{2kT\,Z_{\mathrm{II}}}{P_e Z_{\mathrm{I}}} \left( \frac{2\pi m_e kT}{h^2} \right)^{3/2} e^{-\chi_{\mathrm{I}}/kT}.$$

Using $Z_{\mathrm{I}} = 2.4$ and $Z_{\mathrm{II}} = 1.0$ for the partition functions and $\chi_{\mathrm{I}} = 5.14$ eV for the ionization energy of neutral sodium leads to $N_{\mathrm{II}}/N_{\mathrm{I}} = 2.43 \times 10^3$. There are about 2430 singly ionized sodium atoms for every neutral sodium atom in the Sun's photosphere,[31] so the total number of sodium atoms per unit area above the photosphere is about

$$N = 2430 N_{\mathrm{I}} = 2.43 \times 10^{22}\ \mathrm{m}^{-2}.$$

The mass of a sodium atom is $3.82 \times 10^{-26}$ kg, so the mass of sodium atoms above each square meter of the photosphere is roughly $9.3 \times 10^{-4}$ kg m$^{-2}$. (A more detailed analysis leads to a slightly lower value of $5.4 \times 10^{-4}$ kg m$^{-2}$.) For comparison, the mass of hydrogen atoms per unit area is about 11 kg m$^{-2}$.

---

Thus the number of absorbing atoms can be determined by comparing the equivalent widths measured for different absorption lines produced by atoms or ions initially in the same state (and so having the same column density in the stellar atmosphere) with a theoretical curve of growth. A curve-of-growth analysis can also be applied to lines originating from atoms or ions in different initial states; then applying the Boltzmann equation to the relative numbers of atoms and ions in these different states of excitation allows the excitation temperature to be calculated. Similarly, it is possible to use the Saha equation to find either the electron pressure or the ionization temperature (if the other is known) in the atmosphere from the relative numbers of atoms at various stages of ionization.

[31] The ionization energy for Na II is 47.3 eV. This is sufficiently large to guarantee that $N_{\mathrm{III}} \ll N_{\mathrm{II}}$, so higher states of ionization can be neglected.

### Computer Modeling of Stellar Atmospheres

The ultimate refinement in the analysis of stellar atmospheres is the construction of a *model atmosphere* on a computer. Each atmospheric layer is involved in the formation of line profiles and contributes to the spectrum observed for the star. All of the ingredients of the preceding discussion, plus the equations of hydrostatic equilibrium, thermodynamics, statistical and quantum mechanics, and the transport of energy by radiation and convection, are combined with extensive libraries of opacities to calculate how the temperature, pressure, and density vary with depth below the surface.[32] These models not only provide details regarding line profiles; they also provide information about such fundamental properties as the effective temperature and surface gravity of the star. Only when the variables of the model have been "fine-tuned" to obtain good agreement with the observations can astronomers finally claim to have decoded the vast amount of information carried in the light from a star.

This basic procedure has led astronomers to an understanding of the abundances of the elements in the Sun (see Table 9.2) and other stars. Hydrogen and helium are by far the most common elements, followed by oxygen, carbon, and nitrogen; for every $10^{12}$ atoms of hydrogen, there are $10^{11}$ atoms of helium and about $10^9$ atoms of oxygen. These figures are in very good agreement with abundances obtained from meteorites, giving astronomers

**TABLE 9.2** The Most Abundant Elements in the Solar Photosphere. The relative abundance of an element is given by $\log_{10}(N_{el}/N_H) + 12$. (Data from Grevesse and Sauval, *Space Science Reviews*, *85*, 161, 1998.)

| Element | Atomic Number | Log Relative Abundance |
|---|---|---|
| Hydrogen | 1 | 12.00 |
| Helium | 2 | $10.93 \pm 0.004$ |
| Oxygen | 8 | $8.83 \pm 0.06$ |
| Carbon | 6 | $8.52 \pm 0.06$ |
| Neon | 10 | $8.08 \pm 0.06$ |
| Nitrogen | 7 | $7.92 \pm 0.06$ |
| Magnesium | 12 | $7.58 \pm 0.05$ |
| Silicon | 14 | $7.55 \pm 0.05$ |
| Iron | 26 | $7.50 \pm 0.05$ |
| Sulfur | 16 | $7.33 \pm 0.11$ |
| Aluminum | 13 | $6.47 \pm 0.07$ |
| Argon | 18 | $6.40 \pm 0.06$ |
| Calcium | 20 | $6.36 \pm 0.02$ |
| Sodium | 11 | $6.33 \pm 0.03$ |
| Nickel | 28 | $6.25 \pm 0.04$ |

[32] Details of the construction of a model star will be deferred to Chapter 10.

confidence in their results.[33] This knowledge of the basic ingredients of the universe provides invaluable observational tests and constraints for some of the most fundamental theories in astronomy: the nucleosynthesis of light elements as a result of stellar evolution, the production of heavier elements by supernovae, and the Big Bang that produced the primordial hydrogen and helium that started it all.

## SUGGESTED READING

### General

Hearnshaw, J. B., *The Analysis of Starlight*, Cambridge University Press, Cambridge, 1986.

Kaler, James B., *Stars and Their Spectra*, Cambridge University Press, Cambridge, 1997.

### Technical

Aller, Lawrence H., *The Atmospheres of the Sun and Stars*, Ronald Press, New York, 1963.

Aller, Lawrence H., *Atoms, Stars, and Nebulae*, Third Edition, Cambridge University Press, New York, 1991.

Böhm-Vitense, Erika, "The Effective Temperature Scale," *Annual Review of Astronomy and Astrophysics*, *19*, 295, 1981.

Böhm-Vitense, Erika, *Stellar Astrophysics, Volume 2: Stellar Atmospheres*, Cambridge University Press, Cambridge, 1989.

Cox, Arthur N. (editor), *Allen's Astrophysical Quantities*, Fourth Edition, AIP Press, New York, 2000.

Gray, David F., *The Observation and Analysis of Stellar Photospheres*, Third Edition, Cambridge University Press, Cambridge, 2005.

Grevesse, N., and Sauval, A. J., "Standard Solar Composition," *Space Science Reviews*, *85*, 161, 1998.

Iglesias, Carlos J., and Rogers, Forrest J., "Updated OPAL Opacities," *The Astrophysical Journal*, *464*, 943, 1996.

Mihalas, Dimitri, *Stellar Atmospheres*, Second Edition, W.H. Freeman, San Francisco, 1978.

Mihalas, Dimitri, and Weibel-Mihalas, Barbara, *Foundations of Radiation Hydrodynamics*, Dover Publications, Inc., Mineola, NY, 1999.

Novotny, Eva, *Introduction to Stellar Atmospheres and Interiors*, Oxford University Press, New York, 1973.

Rogers, Forrest, and Iglesias, Carlos, "The OPAL Opacity Code," `http://www-phys.llnl.gov/Research/OPAL/opal.html`.

Rybicki, George B., and Lightman, Alan P., *Radiative Processes in Astrophysics*, John Wiley and Sons, New York, 1979.

[33] A notable exception is lithium, whose solar relative abundance of $10^{1.16}$ is significantly less than the value of $10^{3.31}$ obtained from meteorites. The efficient depletion of the Sun's lithium, sparing only one of every 140 lithium atoms, is probably due to its destruction by nuclear reaction processes when the lithium is transported into the hot interior of the star by convection.

## PROBLEMS

**9.1** Evaluate the energy of the blackbody photons inside your eye. Compare this with the visible energy inside your eye while looking at a 100-W light bulb that is 1 m away. You can assume that the light bulb is 100% efficient, although in reality it converts only a few percent of its 100 watts into visible photons. Take your eye to be a hollow sphere of radius 1.5 cm at a temperature of 37°C. The area of the eye's pupil is about 0.1 $cm^2$. Why is it dark when you close your eyes?

**9.2** **(a)** Find an expression for $n_\lambda \, d\lambda$, the number density of blackbody photons (the number of blackbody photons per $m^3$) with a wavelength between $\lambda$ and $\lambda + d\lambda$.

**(b)** Find the total number of photons inside a kitchen oven set at 400°F (477 K), assuming a volume of 0.5 $m^3$.

**9.3** **(a)** Use the results of Problem 9.2 to find the total number density, $n$, of blackbody photons of all wavelengths. Also show that the average energy per photon, $u/n$, is

$$\frac{u}{n} = \frac{\pi^4 kT}{15(2.404)} = 2.70kT. \tag{9.65}$$

**(b)** Find the average energy per blackbody photon at the center of the Sun, where $T = 1.57 \times 10^7$ K, and in the solar photosphere, where $T = 5777$ K. Express your answers in units of electron volts (eV).

**9.4** Derive Eq. (9.11) for the blackbody radiation pressure.

**9.5** Consider a spherical blackbody of radius $R$ and temperature $T$. By integrating Eq. (9.8) for the radiative flux with $I_\lambda = B_\lambda$ over all outward directions, derive the Stefan–Boltzmann equation in the form of Eq. (3.17). (You will also have to integrate over all wavelengths and over the surface area of the sphere.)

**9.6** Using the root-mean-square speed, $v_{rms}$, estimate the mean free path of the nitrogen molecules in your classroom at room temperature (300 K). What is the average time between collisions? Take the radius of a nitrogen molecule to be 0.1 nm and the density of air to be 1.2 kg $m^{-3}$. A nitrogen molecule contains 28 nucleons (protons and neutrons).

**9.7** Calculate how far you could see through Earth's atmosphere if it had the opacity of the solar photosphere. Use the value for the Sun's opacity from Example 9.2.2 and 1.2 kg $m^{-3}$ for the density of Earth's atmosphere.

**9.8** In Example 9.2.3, suppose that only two measurements of the specific intensity, $I_1$ and $I_2$, are available, made at angles $\theta_1$ and $\theta_2$. Determine expressions for the intensity $I_{\lambda,0}$ of the light above Earth's atmosphere and for the vertical optical depth of the atmosphere, $\tau_{\lambda,0}$, in terms of these two measurements.

**9.9** Use the laws of conservation of relativistic energy and momentum to prove that an isolated electron cannot absorb a photon.

**9.10** By measuring the slope of the curves in Fig. 9.10, verify that the decline of the curves after the peak in the opacity follows a Kramers law, $\overline{\kappa} \propto T^{-n}$, where $n \approx 3.5$.

**9.11** According to one model of the Sun, the central density is $1.53 \times 10^5$ kg $m^{-3}$ and the Rosseland mean opacity at the center is 0.217 $m^2$ $kg^{-1}$.

**(a)** Calculate the mean free path of a photon at the center of the Sun.

**(b)** Calculate the average time it would take for the photon to escape from the Sun if this mean free path remained constant for the photon's journey to the surface. (Ignore the fact that identifiable photons are constantly destroyed and created through absorption, scattering, and emission.)

**9.12** If the temperature of a star's atmosphere is *increasing* outward, what type of spectral lines would you expect to find in the star's spectrum at those wavelengths where the opacity is greatest?

**9.13** Consider a large hollow spherical shell of hot gas surrounding a star. Under what circumstances would you see the shell as a glowing *ring* around the star? What can you say about the optical thickness of the shell?

**9.14** Verify that the emission coefficient, $j_\lambda$, has units of m s$^{-3}$ sr$^{-1}$.

**9.15** Derive Eq. (9.35) in Example 9.4.1, which shows how the intensity of a light ray is converted from its initial intensity $I_\lambda$ to the value $S_\lambda$ of the source function.

**9.16** The transfer equation, Eq. (9.34), is written in terms of the distance, $s$, measured along the path of a light ray. In different coordinate systems, the transfer equation will look slightly different, and care must be taken to include all of the necessary terms.

**(a)** Show that in a spherical coordinate system, with the center of the star at the origin, the transfer equation has the form

$$-\frac{\cos\theta'}{\kappa_\lambda \rho}\frac{dI_\lambda}{dr} = I_\lambda - S_\lambda,$$

where $\theta'$ is the angle between the ray and the outward radial direction. Note that you cannot simply replace $s$ with $r$!

**(b)** Use this form of the transfer equation to derive Eq. (9.31).

**9.17** For a plane-parallel atmosphere, show that the Eddington approximation leads to expressions for the mean intensity, radiative flux, and radiation pressure given by Eqs. (9.46–9.48).

**9.18** Using the Eddington approximation for a plane-parallel atmosphere, determine the values of $I_{\text{in}}$ and $I_{\text{out}}$ as functions of the vertical optical depth. At what depth is the radiation isotropic to within 1%?

**9.19** Using the results for the plane-parallel gray atmosphere in LTE, determine the ratio of the effective temperature of a star to its temperature at the top of the atmosphere. If $T_e = 5777$ K, what is the temperature at the top of the atmosphere?

**9.20** Show that for a plane-parallel gray atmosphere in LTE, the (constant) value of the radiative flux is equal to $\pi$ times the source function evaluated at an optical depth of 2/3:

$$F_{\text{rad}} = \pi S(\tau_v = 2/3).$$

This function, called the **Eddington–Barbier relation**, says that the radiative flux received from the surface of the star is determined by the value of the source function at $\tau_v = 2/3$.

**9.21** Consider a horizontal plane-parallel slab of gas of thickness $L$ that is maintained at a constant temperature $T$. Assume that the gas has optical depth $\tau_{\lambda,0}$, with $\tau_\lambda = 0$ at the top surface of the slab. Assume further that no radiation enters the gas from outside. Use the general solution of the transfer equation (9.54) to show that when looking at the slab from above, you see blackbody radiation if $\tau_{\lambda,0} \gg 1$ and emission lines (where $j_\lambda$ is large) if $\tau_{\lambda,0} \ll 1$. You may assume that the source function, $S_\lambda$, does not vary with position inside the gas. You may also assume thermodynamic equilibrium when $\tau_{\lambda,0} \gg 1$.

**9.22** Consider a horizontal plane-parallel slab of gas of thickness $L$ that is maintained at a constant temperature $T$. Assume that the gas has optical depth $\tau_{\lambda,0}$, with $\tau_\lambda = 0$ at the top surface of the slab. Assume further that incident radiation of intensity $I_{\lambda,0}$ enters the bottom of the slab from outside. Use the general solution of the transfer equation (9.54) to show that when looking at the slab from above, you see blackbody radiation if $\tau_{\lambda,0} \gg 1$. If $\tau_{\lambda,0} \ll 1$, show that you see absorption lines superimposed on the spectrum of the incident radiation if $I_{\lambda,0} > S_\lambda$ and emission lines superimposed on the spectrum of the incident radiation if $I_{\lambda,0} < S_\lambda$. (These latter two cases correspond to the spectral lines formed in the Sun's photosphere and chromosphere, respectively; see Section 11.2.) You may assume that the source function, $S_\lambda$, does not vary with position inside the gas. You may also assume thermodynamic equilibrium when $\tau_{\lambda,0} \gg 1$.

**9.23** Verify that if the source function is $S_\lambda = a_\lambda + b_\lambda \tau_{\lambda,v}$, then the emergent intensity is given by Eq. (9.57), $I_\lambda(0) = a_\lambda + b_\lambda \cos\theta$.

**9.24** Suppose that the shape of a spectral line is fit with one-half of an ellipse, such that the semimajor axis $a$ is equal to the maximum depth of the line (let $F_\lambda = 0$) and the minor axis $2b$ is equal to the maximum width of the line (where it joins the continuum). What is the equivalent width of this line? *Hint:* You may find Eq. (2.4) useful.

**9.25** Derive Eq. (9.60) for the uncertainty in the wavelength of a spectral line due to Heisenberg's uncertainty principle.

**9.26** The two solar absorption lines given in Table 9.3 are produced when an electron makes an upward transition from the ground state orbital of the neutral Na I atom.

**(a)** Using the general curve of growth for the Sun, Fig. 9.22, repeat the procedure of Example 9.5.5 to find $N_a$, the number of absorbing sodium atoms per unit area of the photosphere.

**(b)** Combine your results with those of Example 9.5.5 to find an average value of $N_a$. Use this value to plot the positions of the four sodium absorption lines on Fig. 9.22, and confirm that they do all lie on the curve of growth.

**9.27** Pressure broadening (due to the presence of the electric fields of nearby ions) is unusually effective for the spectral lines of hydrogen. Using the general curve of growth for the Sun with these broad hydrogen absorption lines will result in an overestimate of the amount of hydrogen present. The following calculation nevertheless demonstrates just how abundant hydrogen is in the Sun.

The two solar absorption lines given in Table 9.4 belong to the Paschen series, produced when an electron makes an upward transition from the $n = 3$ orbital of the hydrogen atom.

**(a)** Using the general curve of growth for the Sun, Fig. 9.22, repeat the procedure of Example 9.5.5 to find $N_a$, the number of absorbing hydrogen atoms per unit area of the photosphere (those with electrons initially in the $n = 3$ orbital).

**(b)** Use the Boltzmann and Saha equations to calculate the total number of hydrogen atoms above each square meter of the Sun's photosphere.

**TABLE 9.3** Data for Solar Sodium Lines for Problem 9.26. (Data from Aller, *Atoms, Stars, and Nebulae*, Revised Edition, Harvard University Press, Cambridge, MA, 1971.)

| $\lambda$ (nm) | $W$ (nm) | $f$ |
|---|---|---|
| 330.298 | 0.0067 | 0.0049 |
| 589.594 | 0.0560 | 0.325 |

**TABLE 9.4** Data for Solar Hydrogen Lines for Problem 9.27. (Data from Aller, *Atoms, Stars, and Nebulae*, Revised Edition, Harvard University Press, Cambridge, MA, 1971.)

| $\lambda$ (nm) | $W$ (nm) | $f$ |
|---|---|---|
| 1093.8 (Pa$\gamma$) | 0.22 | 0.0554 |
| 1004.9 (Pa$\delta$) | 0.16 | 0.0269 |

## COMPUTER PROBLEMS

**9.28** In this problem, you will use the values of the density and opacity at various points near the surface of the star to calculate the optical depth of these points. The data in Table 9.5 were obtained from the stellar model building program `StatStar`, described in Section 10.5 and Appendix L. The first point listed is at the surface of the stellar model.

**(a)** Find the optical depth at each point by numerically integrating Eq. (9.15). Use a simple trapezoidal rule such that

$$d\tau = -\kappa\rho\, ds$$

becomes

$$\tau_{i+1} - \tau_i = -\left(\frac{\kappa_i\rho_i + \kappa_{i+1}\rho_{i+1}}{2}\right)(r_{i+1} - r_i)\,,$$

where $i$ and $i+1$ designate adjacent zones in the model. Note that because $s$ is measured along the path traveled by the photons, $ds = dr$.

**(b)** Make a graph of the temperature (vertical axis) vs. the optical depth (horizontal axis).

**(c)** For each value of the optical depth, use Eq. (9.53) to calculate the temperature for a plane-parallel gray atmosphere in LTE. Plot these values of $T$ on the same graph.

**(d)** The `StatStar` program utilizes a simplifying assumption that the surface temperature is zero (see Appendix L). Comment on the validity of the surface value of $T$ that you found.

**9.29** The binary star code `TwoStars`, discussed in Section 7.3 and Appendix K, makes use of an empirical limb darkening formula developed by W. Van Hamme (*Astronomical Journal, 106*, 1096, 1993):

$$\frac{I(\theta)}{I(\theta = 0)} = 1 - x(1 - \cos\theta) - y\cos\theta\, \log_{10}(\cos\theta),$$

where $x = 0.648$ and $y = 0.207$ for solar-type stars (other coefficients are provided for other types of stars).

**(a)** Plot Van Hamme's formula for limb darkening over the range $0 \leq \theta \leq 90°$. (Be sure to correctly treat the singularity in the function at $\theta = 90°$.)

**(b)** Plot Eq. (9.58), which is based on the Eddington approximation, on the same graph.

**(c)** Where is the difference between the two formulae the greatest?

**(d)** Compare the two curves to the observational data shown in Fig. 9.17. Which curve best represents the solar data?